Review Article. Tribute to Founders: Neal R. Amundson. Reaction Engineering, Kinetics, and Catalysis

Energy Generation Using Thermopower Waves: Experimental and Analytical Progress

Sayalee G. Mahajan, Qing Hua Wang, and Michael S. Strano
Dept. of Chemical Engineering, 77 Massachusetts Avenue, Massachusetts Institute of Technology, Cambridge, MA 02139

Joel T. Abrahamson
Dept. of Chemical Engineering and Materials Science, University of Minnesota, Twin Cities, Minneapolis MN 55455

DOI 10.1002/aic.14143
Published online July 15, 2013 in Wiley Online Library (wileyonlinelibrary.com)

Thermopower waves convert chemical energy into electrical power using nanostructured thermal conduits like carbon nanotubes (CNTs) by taking advantage of their high thermal conductivity to propagate the heat released by an exothermic reaction of a fuel layer coated around the conduit. Electron–phonon coupling in the CNTs then leads to an electrical output. Previous work using cyclotrimethylene-trinitramine coated around multiwalled CNTs has shown electrical output as high as 7 kW kg^{-1}. This phenomenon has potential to aid the manufacture of nanoscale power sources capable of releasing large power pulses for specific applications. Researchers have studied the effects of other system properties, including the conduit thermal conductivity, the chemical properties of the fuel, and the coupling of the reactions to inorganic thermoelectric materials. An analytical solution for the governing heat and mass balance equations has also been derived. Here, we review the progress made in the field of thermopower waves. © 2013 American Institute of Chemical Engineers *AIChE J*, 59: 3333-3341, 2013
Keywords: carbon nanotubes, thermopower, power source, thermoelectric materials

Introduction

Neal R. Amundson (1916–2011) is considered to have been one of the most prominent chemical engineering educators in United States. He is known for his pioneering work in the field of modeling chemical reactors, separation systems, and combustion of coal.[1] The concept of thermopower waves has benefited enormously from progress in these areas. Thermopower waves involve coupling the exothermic nature of a chemical reaction with advantageous electrical and thermal properties of the conduit on which the reaction is carried out. It is a novel means of obtaining electrical output using a thermal gradient, beyond what is possible via the conventional thermoelectric effect.

The conventional Seebeck effect or thermoelectric effect describes the phenomenon of electric output generated by a temperature difference across the ends of a thermoelectric material. The output voltage ΔV as a function of the temperature gradient is given by the relation

$$\Delta V = \int_{T_{\text{left}}}^{T_{\text{right}}} \Gamma_s \ \nabla T \tag{1}$$

where Γ_s is the Seebeck coefficient. Exploiting the traditional Seebeck effect requires thermoelectric materials having high electrical conductivity σ to enhance electron transport, but low thermal conductivity k to maintain the temperature difference across the ends of the device. The suitability of a material for thermoelectric applications is measured by means of "the figure of merit" ZT, defined as[2]

$$\mathrm{ZT} = \frac{\Gamma_s \sigma \ T}{k} \tag{2}$$

The higher the value of ZT, the better suited is the material for thermoelectric applications.

Basics of Thermopower Waves

Thermopower waves rely on exploiting the effect of carrying out an exothermic chemical reaction on a conduit with improved electrical and thermal properties. Thermopower waves were first demonstrated using carbon nanotubes (CNTs) as the conduit material. CNTs are one-dimensional molecular structures having high thermal conductivity of the order of 3000 W m^{-1} K^{-1} and possessing electrical conductivity of around 10^6 S m^{-1}.[2] The high thermal conductivity renders CNTs less effective for traditional Seebeck applications. However, the phenomenon of thermopower waves effectively exploits this property to drive the heat from the exothermic fuel reaction along the length of the nanotubes.

Correspondence concerning this article should be addressed to M. S. Strano at strano@MIT.edu.

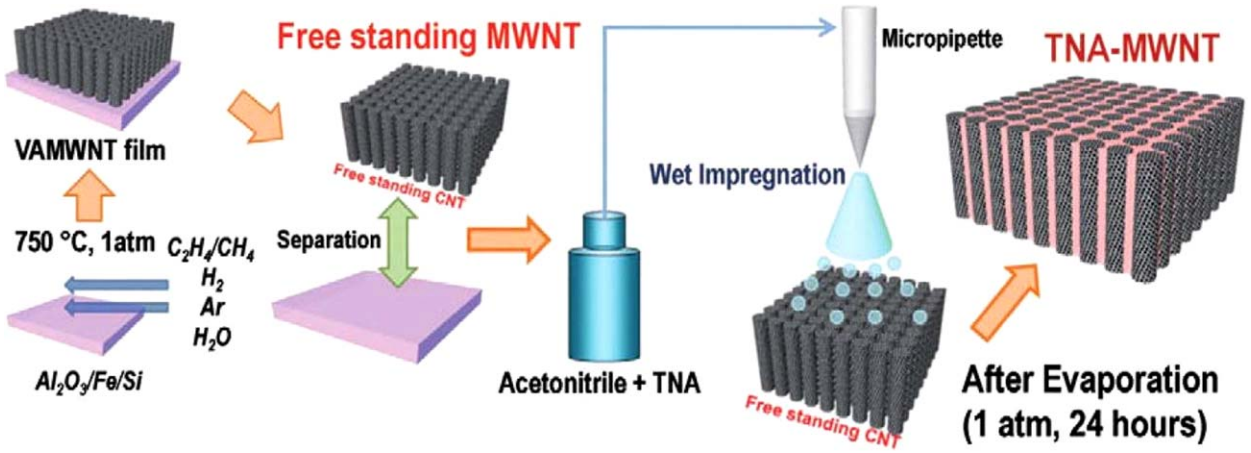

Figure 1. Schematic of the production of CNT-based thermopower wave generators using TNA solution in acetonitrile.[2]

Reproduced and adapted from Ref 2, with permission from Elsevier Ltd. [Color figure can be viewed in the online issue, which is available at wileyonlinelibrary.com.]

The preparation of a thermopower generator (TWG) device involves coating a layer of fuel (cyclotrimethylenetrinitramine (TNA) in the example of Figure 1) onto a conduit. The schematic depicts multiwalled carbon nanotubes (MWCNTs) as the conduit, although single-walled nanotubes (SWNTs) also support thermopower waves.[3,4] The fuel, TNA, is dissolved in acetonitrile, impregnated into the MWCNT array, and allowed to dry.[2] A small amount of an initiator, in this case sodium azide (NaN_3), is also added because it reacts exothermically with a lower energy of activation, thus requiring less input energy. The chemical structures of fuels, NaN_3, and acetonitrile used in TWGs are shown in Figure 2. As shown in Figure 3, in a TWG, the fuel-coated conduits are connected to copper tape electrodes with silver paste.

A thermopower wave is initiated with an external ignition source such as a butane torch, joule heater, or laser, helping the sodium azide overcome its reaction barrier.[2] Exothermic reaction of sodium azide provides initiation for the fuel reaction. The fuel reacts and releases heat, which is then accelerated forward because of the high thermal conductivity of the CNTs. This heat now ignites the fuel that lies in its path, and thus a continuous reaction wave is sustained. Figure 4 shows a schematic of how heat propagates in a CNT–TNA system once a self-propagating TNA reaction wave is launched.

Because of electron-phonon coupling exhibited by CNTs, we also obtain an electrical output.[3] Examples of experimentally obtained voltage outputs are shown in Figure 5. Depending on the direction of the wave propagation, the polarity of the voltage can be positive or negative.[3]

Covalently Functionalized CNTs as Thermopower Conduits

Diazonium chemistry was used to synthesize single-walled CNTs decorated with mono-, di-, and trinitrobenzenes, with the purpose of increasing the energy density of the CNTs.[4] Differential scanning calorimetry revealed the effect of covalent functionalization of nanotubes on the reaction activation energy, which was lower at lower values of conversion. Covalent bonds to the nanotube lattice can create defects that tend to scatter electrons and phonons, and thus, reduce electrical and thermal conductivity, both of which are essential for thermopower wave propagation. Figure 6 shows the increase in the disorder (D) mode in Raman spectroscopy due to covalent functionalization of nanotubes. Fourier Transform -Infrared (FT-IR) spectra confirmed attachment of nitro groups on these CNTs.[4]

Work by Chakraborty et al. shows that electrical resistivity of single-walled CNTs increases almost three-fold post functionalization by mononitrophenyl (MNP).[5] Heating the samples to 500°C under ultra-high vacuum showed the electronic changes caused by functionalization to be reversible.[5] Thermopower experiments, however, showed that it was possible to launch thermopower waves and produce electrical power from such nitrobenzene functionalized conduits. The electrical power generated was affected little by functionalization. Also, both the reaction wave velocity and the specific power did not show a drastic decrease after functionalization. Thus, though the electrical[5] and thermal conductivities of functionalized CNTs might be lower than that of bare CNTs, the values are still high enough to allow propagation of a thermopower wave. Raman spectroscopy on functionalized conduit samples

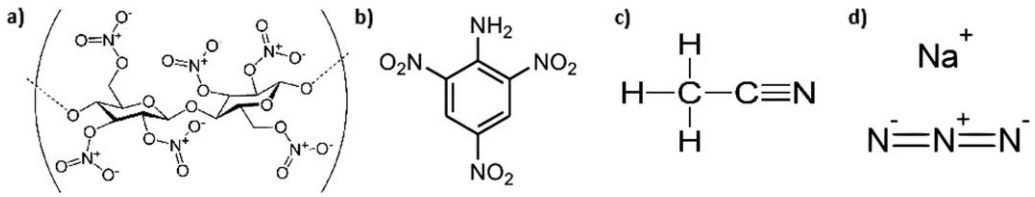

Figure 2. Chemical structures of compounds used for thermopower waves experiments.

(a) Nitrocellulose (b) 2, 4, 6-Trinitroaniline or picramide (c) Acetonitrile (d) Sodium Azide.

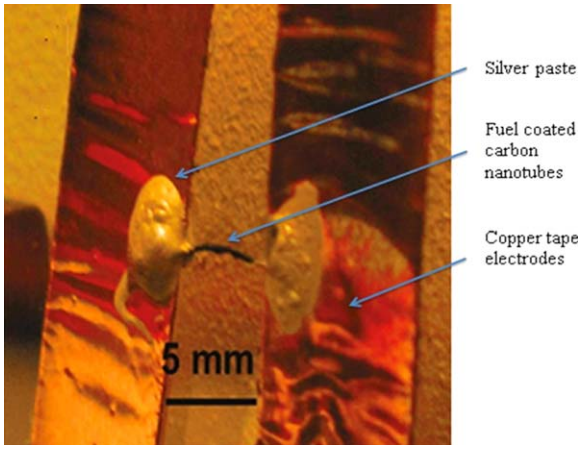

Figure 3. A typical TWG consisting of fuel-coated CNTs.[4]

Silver paste is used to connect CNTs to copper tape electrodes, through which an oscilloscope can measure voltage output. Reproduced and adapted from Ref 4, with permission from American Chemical Society. [Color figure can be viewed in the online issue, which is available at wileyonlinelibrary.com.]

before and after thermopower wave reaction shows a reduction in the ratio of intensity of D peak to G peak, that is, D/G ratio after the reaction wave has passed over the conduit. D/G ratio is indicative of the number of defects present in the sample being analyzed. Through this Raman analysis, we can infer that reaction wave breaks the covalent bonds attaching the functional groups to the CNTs, thus leading to fewer defects after reaction.

The Effect of Thermal Conductivity of Thermopower Conduits

The effect of thermal conduits of different values of thermal conductivity has been studied. Terracotta ($k = 1$ W m^{-1} K^{-1}, low thermal conductivity) and alumina, Al_2O_3 ($k = 20$ W m^{-1} K^{-1}, comparatively higher thermal conductivity) were chosen for the comparison.[6] Additionally, a layer of Bi_2Te_3 (bismuth telluride), a thermoelectric material, was deposited on top of the thermal conduit to generate voltage from its high Seebeck coefficient (287 μV K^{-1}) and high electrical conductivity on the order of 10^5 S m^{-1}.[6,7] The Bi_2Te_3 layer must be thin for the heat transfer to be dominated by the thicker conduit layer beneath it. The fuel layer is deposited on top of the Bi_2Te_3 for direct heating and maximal voltage generation. These devices are shown schematically in Figure 7.

Thermopower wave experiments using both the conduits were carried out and the voltage output and wave velocity studied. Bi_2Te_3 films were sputtered onto both the conduits. Nitrocellulose was used as fuel and NaN_3 was used as initiator for the reaction.[6] Experiments using the Al_2O_3 conduit showed oscillations in velocity and voltage. The average velocity of these waves was around 0.01–0.9 m s^{-1}, with the median value being around 0.4 m s^{-1}.[6] These large velocity devices generated voltages in the range of 40–150 mV, with power output up to 10 mW. Experiments with varying mass of fuel showed 24–27 mg of fuel to be the optimum range to obtain maximum voltage and power.[6] Study of systems using terracotta as conduit showed no oscillations in wave velocity, with average value of velocity around 0.01 m s^{-1}.[6] Thus, wave velocity of the self-propagating reaction wave and presence or absence of oscillations in velocity and voltage output was found to be highly dependent on the thermal conductivity of the conduit being used. In the forthcoming section, we discuss the analytical solution studying the dependence of wave velocity on thermal conductivity of the conduit and how well it matches with the experimental observations. Also, a study of effect of thickness of the thermoelectric layer showed that both 10 μm and 5 μm thick Bi_2Te_3 films showed similar trends in the voltage generated. Voltage output from the 10 μm Bi_2Te_3 device was slightly higher because of increased sheet resistance as compared to the thinner Bi_2Te_3 layer.[6] Bi_2Te_3 layers thicker than about 30 μm when sputtered onto Al_2O_3 reduced the overall thermal conductivity leading to no oscillations in the voltage output.

Effects of P-type and N-type Thermoelectric Materials in Thermopower Conduits

To exploit thermoelectric materials with higher Seebeck coefficients than that of CNTs, TWGs were made with bismuth telluride (Bi_2Te_3), an n-type thermoelectric (Seebeck coefficient = 287 μV K^{-1}), and antimony telluride (Sb_2Te_3), a p-type thermoelectric (Seebeck coefficient = 243 μV K^{-1}), referring to their majority carriers of electrons and holes, respectively.[6] Here again, experiments were repeated with two base thermal conduits, alumina and terracotta. The

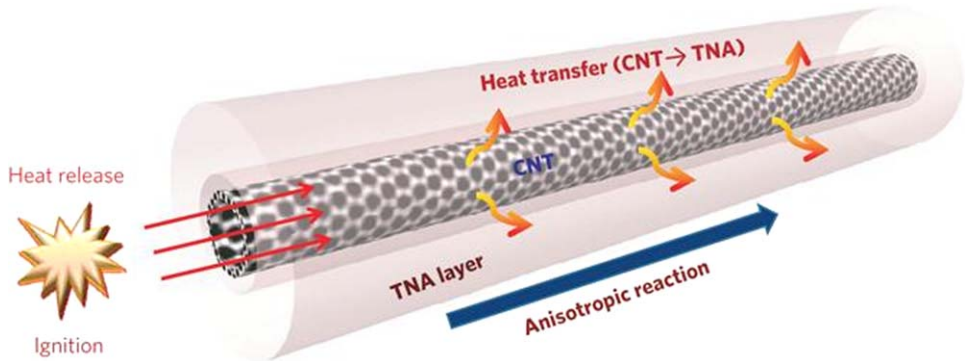

Figure 4. Schematic of the principle of thermopower waves.

A self-propagating reaction wave is initiated by means of a heat source and is sustained because of high thermal conductivity of CNTs.[3] Reproduced and adapted from Ref 3, with permission from Nature Publishing Group. [Color figure can be viewed in the online issue, which is available at wileyonlinelibrary.com.]

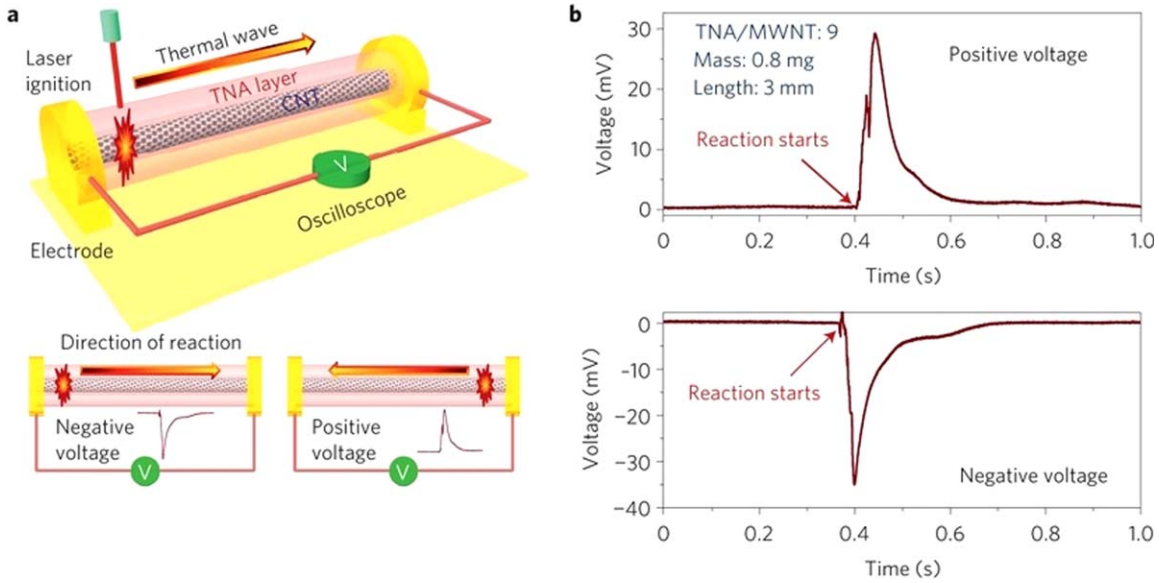

Figure 5. Electrical output obtained by operation of a thermopower wave device.

(a) Schematic of a thermopower waves device and dependence of the voltage output polarity on the reaction wave direction. (b) Actual voltages obtained during thermopower waves experiments.[3] Reproduced and adapted from Ref 3, with permission from Nature Publishing Group. [Color figure can be viewed in the online issue, which is available at wileyonlinelibrary.com.]

experimental setup is similar to that shown in Figure 7a. Changing the type of thermoelectric reverses the polarity of the voltage output. As observed before, using nitrocellulose with sodium azide as the fuel and alumina as the conduit generated oscillating voltage for the duration of wave propagation.[6] Figure 8 shows typical voltage outputs from both thermoelectric materials. Reaction waves on Sb_2Te_3 are faster, with mean reaction propagation velocities of about 660 mm s^{-1} compared to about 210 mm s^{-1} for Bi_2Te_3 devices.[7] This was attributed to Sb_2Te_3 having a thermal conductivity that is almost 2.5 times that of Bi_2Te_3.

Both Sb_2Te_3 and Bi_2Te_3 systems produced high-power pulses, 0.6 kW kg^{-1} and 1.0 kW kg^{-1}, respectively.[7] This work shows that certain conduit properties can lead to oscillating voltage.[6,7] It also opens avenues for generating alternating voltage output from thermopower wave devices by using p-type and n-type semiconductors simultaneously as conduits.

ZnO Thermal Conduits

Recent work incorporated zinc oxide in a TWG device. ZnO has a high Seebeck coefficient of about -360 μV K^{-1} at 85°C, high thermal conductivity of about 15 W m^{-1} K^{-1} at 300°C, and high electrical conductivity at elevated temperatures.[8] A ZnO film was deposited on an alumina conduit, followed by a fuel layer of nitrocellulose and sodium azide. The reaction was initiated using a fine-tip butane torch, and produced voltage pulses as large as 500 mV.[8] Here again, wave propagation gave rise to oscillating voltage output. Power output from some devices was as high as 1 mW with device efficiencies around 0.2%.[8]

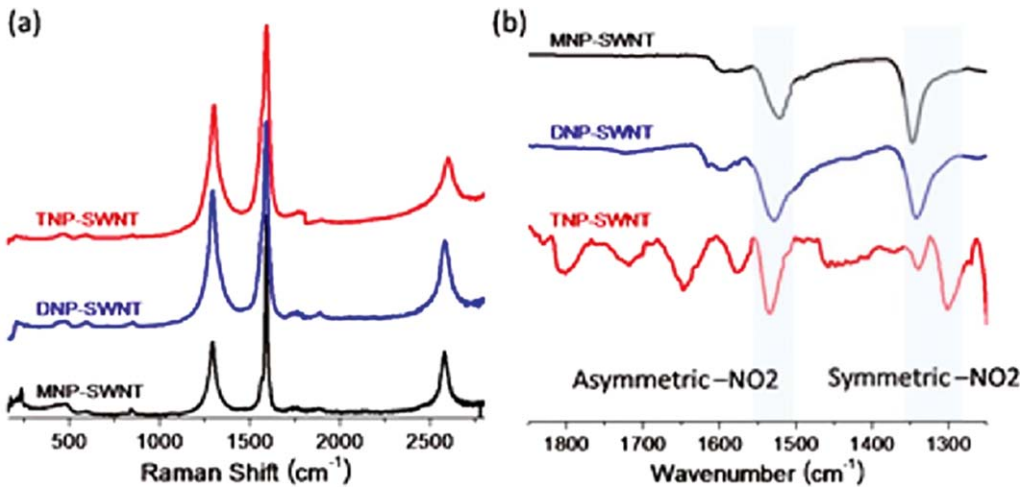

Figure 6. Raman and FT-IR analysis of energetically decorated SWNTs.

(a) Raman spectra show an increase in disorder modes (i.e. peak at ~1350 cm^{-1}) after covalent functionalization with any of three nitrophenyl species. (b) FT-IR spectra using ATR (attenuated total reflectance) confirmed presence of nitro groups in thin films. MNP-, DNP-, and TNP-SWNTs stand for mono-, di-, and trinitrophenyl-functionalized SWNTs, respectively.[4] Reproduced from Ref 4, with permission from American Chemical Society. [Color figure can be viewed in the online issue, which is available at wileyonlinelibrary.com.]

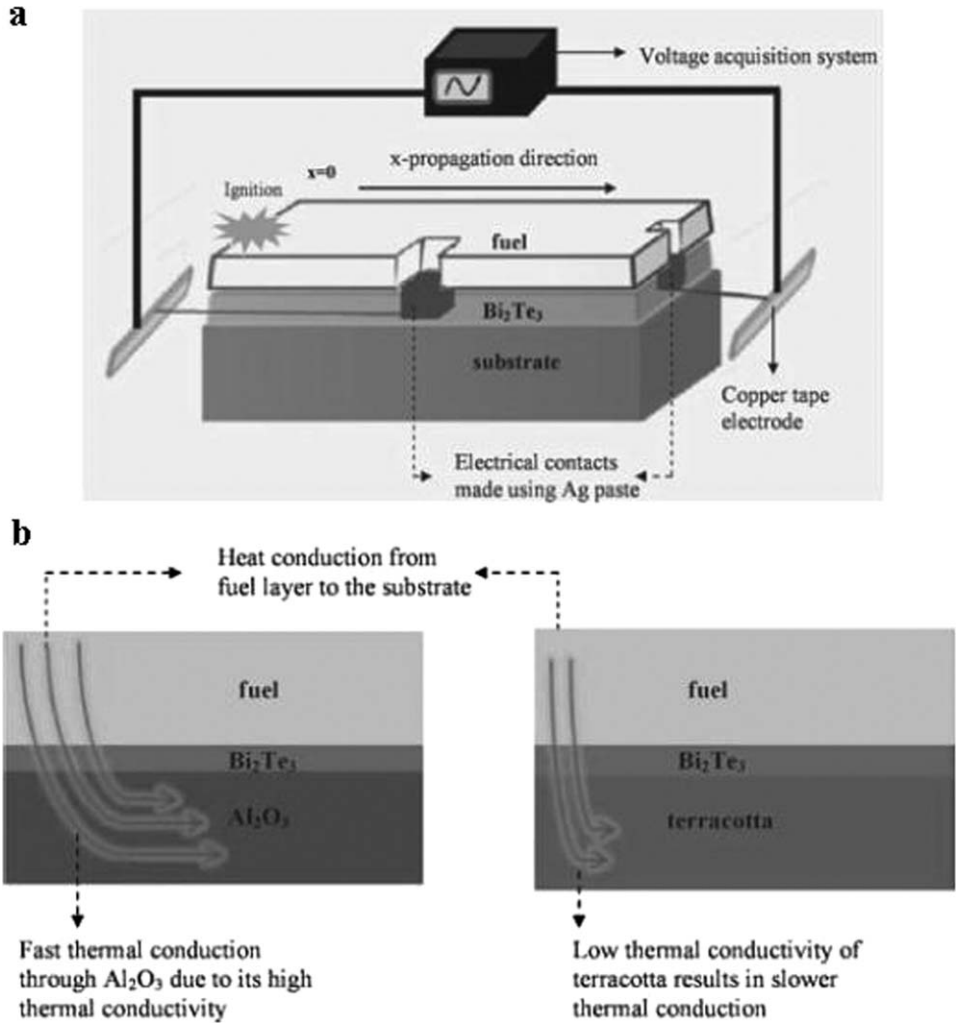

Figure 7. Nitrocellulose/Bi_2Te_3/Thermal conduit configuration for thermopower waves studies.

(a) Schematic of experimental setup. (b) Schematic of heat conduction from the fuel to the conduit layer and the effects of conduit thermal conductivity.[6] Reproduced from Ref 6, with permission from John Wiley and Sons.

The efficiency of a TWG device is the ratio of the electrical power output to the heat energy released from the exothermic chemical reaction.

$$\%\,\text{Efficiency} = \frac{\text{Electrical energy output}}{\text{Energy released due to the fuel chemical reaction}} \times 100 = \frac{\int\left(\frac{V^2}{R_c}\right)dt}{m(-\Delta H)} \times 100 \tag{3}$$

Here, V is the voltage output, R_c is the circuit load, m is the mass of the fuel reacting and $(-\Delta H)$ is the exothermic heat of reaction. Although the overall energy conversion efficiency of TWG devices is $<1\%$, they are able to provide large voltage pulses for applications requiring energy to be released over short durations, unlike batteries or fuel cells.

Analytical Solution of Equations Governing One-Dimensional Thermopower Waves

The governing analytical equations of thermopower waves have been further studied. For solid fuels, the mass diffusion is negligible, and hence, that term can be neglected. Using a reaction term with a first-order Arrhenius form for the fuel and using Fourier's law for heat diffusion, coupled heat and mass balance equations can be set up as below:

$$\rho C_p \frac{\partial T}{\partial t} = k\frac{\partial^2 T}{\partial x^2} - (\Delta H.\ k_o Y)e^{-\frac{E_a}{RT}} \tag{4}$$

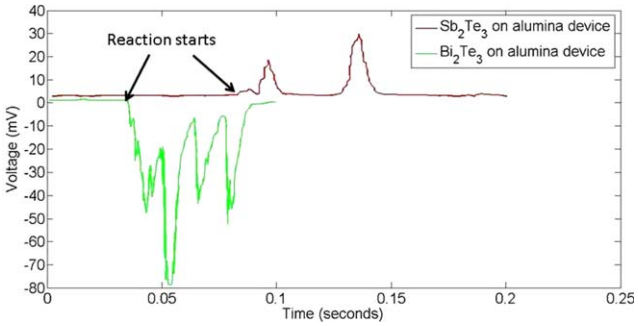

Figure 8. Oscillatory voltage output from thermopower waves devices using Sb_2Te_3 on alumina and using Bi_2Te_3 on alumina.

Adapted from Ref 7. [Color figure can be viewed in the online issue, which is available at wileyonlinelibrary.com.]

$$\frac{\partial Y}{\partial t} = -(\ k_o Y) e^{-\frac{E_a}{RT}} \tag{5}$$

Here, ρ is the fuel density, T is the temperature, C_p is the specific heat of the fuel, k is fuel thermal conductivity, x is the distance or space coordinate, $(-\Delta H)$ is the exothermic heat of reaction, k_0 is Arrhenius prefactor, E_a is the activation energy of the fuel reaction, R is the universal gas constant and Y is mass concentration of the fuel.[9] Coupled heat and mass balance equations are widely applicable to many other fields, such as high-temperature self-propagating synthesis reactions. Nondimensionalizing the above set of equations simplifies them:

$$\frac{\partial u}{\partial \tau} = \frac{\partial^2 u}{\partial \xi^2} + y e^{-\frac{1}{u}} \tag{6}$$

$$\frac{\partial y}{\partial \tau} = -\ \beta y e^{-\frac{1}{u}} \tag{7}$$

Here, $u=(R/E_a)T$ is the nondimensional temperature and $y=Y/\rho$ is the nondimensional fuel concentration. Similarly, $\xi = x\left[\left(\frac{\rho C_p}{k}\right)\left(\frac{(-\Delta H)k_o R}{C_p E_a}\right)\right]^{1/2}$ is the nondimensional space coordinate and $\tau = \left(\frac{(-\Delta H)k_o R}{C_p E_a}\right)t$ is the nondimensional time. The new parameter that arises due to this nondimensionalization is $\beta = \frac{C_p E_a}{(-\Delta H)R}$. β corresponds to the (dimensionless) inverse adiabatic reaction temperature rise, the temperature behind the wave front during steady-state adiabatic reaction wave propagation. Thus, ideally, the temperature difference that leads to the traditional Seebeck voltage output from thermopower wave generators is $1/\beta$. Solving the above nondimensional Eqs. 6 and 7 using numerical methods and assuming ideal adiabatic boundary conditions showed the temperature profiles $u(\xi)$ to be unchanging in shape with respect to time.[9–11] Examples of the numerically calculated temperature profile as a function of time and space are shown in Figure 9.

The waves propagate with constant velocity for certain values of β. In order to solve this equation, a new variable η was introduced to combine the time and distance of propagation.

$$\eta = \xi - c\tau \tag{8}$$

Here c is the constant wave velocity.

A logistic wave function can describe the wave form observed during numerical simulations. Thus, we set

$$u(\eta) = \frac{u_{max}}{(1+Qe^{s\eta})^{1/Q}} \tag{9}$$

Here, u_{max} is the maximum temperature behind the reaction wave front, and s is a parameter that affects the slope of the u growth. Q is a symmetry parameter and affects the curvature of the function near asymptotes. As mentioned before, $u_{max} = {}^{1}/_{\beta}$, which corresponds to the maximum possible temperature behind the wave front in event of adiabatic boundary conditions. On substituting this in the above set of nondimensional equations, an equation for wave velocity was obtained:

$$c = e^{-\left(\frac{\beta}{2}\right)(1+Q)^{\frac{1}{Q}}} \sqrt{\left(\frac{\beta}{Q}\right)\left(-1+(1+Q)^{(1+Q)/Q}\right)} \tag{10}$$

This equation holds for first-order fuel reactions. One can then solve for $Q(\beta)$. An expression was obtained by empirical fitting.[9]

$$Q = 0.0061\beta^3 - 0.077\beta^2 + 1.2531\beta - 0.208 \tag{11}$$

The temperature profiles obtained from numerical solution and from the logistic form analytical solution are compared in Figure 10. A coupled system of heat and mass transfer equations under adiabatic boundary conditions is well described by the logistic functional form, especially for smaller β values. Above $\beta = 6$, the logistic form becomes less accurate as the wave velocity is no longer constant.

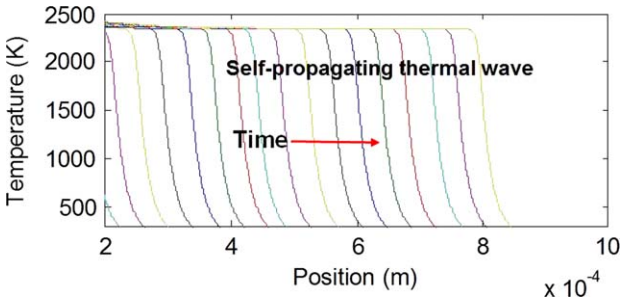

Figure 9. Examples of numerically simulated temperature waves. The different color curves in the diagram represent the temperature at different time points.

[Color figure can be viewed in the online issue, which is available at wileyonlinelibrary.com.]

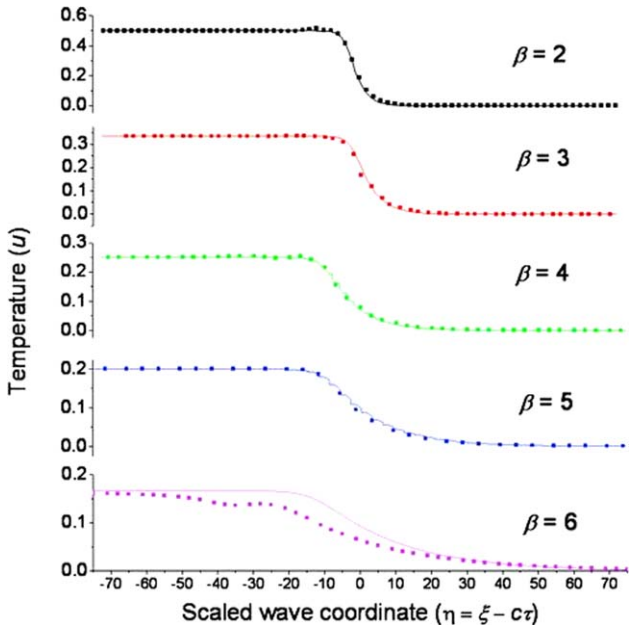

Figure 10. Analytical and numerical solutions using a logistic temperature profile.

Analytical solutions are represented by lines, numerical solutions by points. The profiles match closely for several different values of β.[9] Reproduced from Ref 9, with permission from American Chemical Society. [Color figure can be viewed in the online issue, which is available at wileyonlinelibrary.com.]

Velocity Oscillations in Thermopower Waves

The system of coupled heat and mass transfer equations shown above is a simplified set of equations considering the balances for only the fuel. A more rigorous approach incorporates the heat balance for the conduit as well. The nondimensional equations used here are:

$$\frac{\partial u}{\partial \tau} = \frac{\partial^2 u}{\partial \xi^2} + (1-\omega)e^{-\frac{1}{u}} - \gamma_1(u-u_2) \tag{12}$$

$$\frac{\partial u_2}{\partial \tau} = \alpha_0 \frac{\partial^2 u_2}{\partial \xi^2} + \gamma_2(u-u_2) \tag{13}$$

$$\frac{\partial \omega}{\partial \tau} = \beta(1-\omega)e^{-\frac{1}{u}} \tag{14}$$

Here, u is the fuel temperature, u_2 is the conduit temperature and ω is the fuel amount that has been consumed i.e. $\omega = 1-y$. τ, ξ and β have same meaning as before. γ_1, γ_2, and α_0 depend on system properties like fuel and conduit thermal conductivities, interfacial conductance between the fuel and the conduit, conduit diameter, diameter of the fuel-conduit system, β, their densities and their molecular weights.[12]

Terms for heat transfer between the fuel layer and the CNTs must be included with a term for interfacial energy exchange.[12] With added complexity, the analytical solution above does not hold and the equations must be solved numerically to evaluate the wave velocity. This analysis shed light on the interesting phenomenon of oscillating wave velocity. Increasing β leads to increased amplitude of velocity oscillations but decreased fundamental frequency.[12] Wave front velocity simulations were carried out on a system of CNT wrapped by a TNA layer. Figure 11 shows results from this study where wave front velocity is studied as a function of β. As can be seen from the figure, the average velocity decreased with increase in β from 4 to 9. The nature of the velocity profile also undergoes drastic change as β changes. Starting with low amplitude velocity oscillations, the velocity becomes almost constant at about $\beta = 6$. Beyond $\beta = 7$, the wave velocity starts showing oscillations with varying regions of velocity having different frequencies of oscillations.

Experimentally, β can be adjusted by changing the fuel. Experiments with TNA on MWCNTs confirmed the theory of velocity oscillations,[12] followed by nitrocellulose with NaN_3 on Bi_2Te_3/alumina.[6] The output voltage and wave velocity were correlated, with voltage oscillating during wave propagation, followed by a smooth return to baseline during conduit cooling. These results provide scope for developing nanoscale power sources with oscillating single polarity voltage by using appropriate combinations of fuel and conduit.

To explore the effects of the thermal conduit on the magnitude of voltage oscillations, the earlier work using Bi_2Te_3/alumina and Bi_2Te_3/terracotta conduits was also studied analytically with a system of nondimensional heat and mass balance equations, similar to Eqs. 6 and 7.[6] However, this analysis also included a parameter accounting for heat transfer from fuel to the conduit and the surroundings, so the system was not adiabatic. The modified nondimensional equations are:

$$\frac{\partial u}{\partial \tau} = \frac{\partial^2 u}{\partial \xi^2} + ye^{-\frac{1}{u}} - l(u-u_a) \tag{15}$$

$$\frac{\partial y}{\partial \tau} = -\beta y e^{-\frac{1}{u}} \tag{16}$$

Here, l is a parameter for nondimensional heat transfer and u_a is the ambient nondimensional temperature. Also,

$$l = \frac{hSE_a}{VR\rho(-\Delta H)k_0} \tag{17}$$

Here, h is the heat-transfer coefficient from the fuel to the surrounding and S/V is the surface area to volume ratio for the fuel.[6] Theoretical calculations yielded the combination of β and l values that lead to oscillations. Simulations showed that the conduit with higher thermal conductivity (alumina) showed oscillations in velocity, unlike the lower thermal conductivity conduit (terracotta). Also, an analytical expression obtained from literature was used to predict the wave velocity for terracotta conduit systems.[6]

$$c - \frac{l}{c} = \frac{1}{c}e^{-\beta}\left(e^{2l\beta/c^2} - e^{-\beta}\right) \tag{18}$$

Here, c is the wave velocity in m s^{-1}. Predicted and experimental wave velocities matched to an order of magnitude. Using Eq. 18, average wave velocity was estimated to be around 0.007 m s^{-1} for Bi_2Te_3/terracotta system used with nitrocellulose and sodium azide fuel. As predicted by theory, experiments showed low and nonoscillating reaction wave velocities for fuel/Bi_2Te_3/terracotta systems, with wave velocity of the order of magnitude of 0.01 m s^{-1}.[6] Thermopower waves propagate at 0.4 m s^{-1} in the Bi_2Te_3/alumina system, with oscillations observed for samples with lower thickness of Bi_2Te_3 layers.[6]

Theory of Excess Thermopower: Advantages of Thermopower Waves Over Traditional Thermoelectric Materials

In most TWG devices, despite using conduits such as CNTs with a relatively low Seebeck coefficient, the Seebeck effect still contributes somewhat to the output voltage during the exothermic fuel reactions. For $T_{rxn} \sim 1100$ K, which is representative of theoretical temperatures attained during thermopower experiments using nitrocellulose fuel, a traditional Seebeck effect alone would produce about 11 mV using CNTs.[13] This is much lower than typical voltage outputs of thermopower waves devices, which can generate voltage up to 220 mV using CNT conduits.[13] Mathematically, the Seebeck effect expression is derived from Boltzmann transport equation for carriers:

$$J = \sigma_h\left(E + \frac{\Delta\mu}{e}\right) - L_{12}\nabla T \tag{19}$$

where J is current density, σ_h is electrical conductivity, E is electric field, μ is chemical potential, e is the elementary charge, L_{12} is an Onsager coupling coefficient, and T is temperature. In the conventional thermoelectric treatment, in the limit of zero current density, we obtain

$$V = \int_{x_L}^{x_R}\left(\frac{\Delta\mu}{e} - \frac{L_{12}}{\sigma_h}\nabla T\right)dx \tag{20}$$

Here, V is the voltage difference and x_L and x_R represent the positions for electrical measurements at the two ends of the device. Most of the experiments in thermoelectricity do

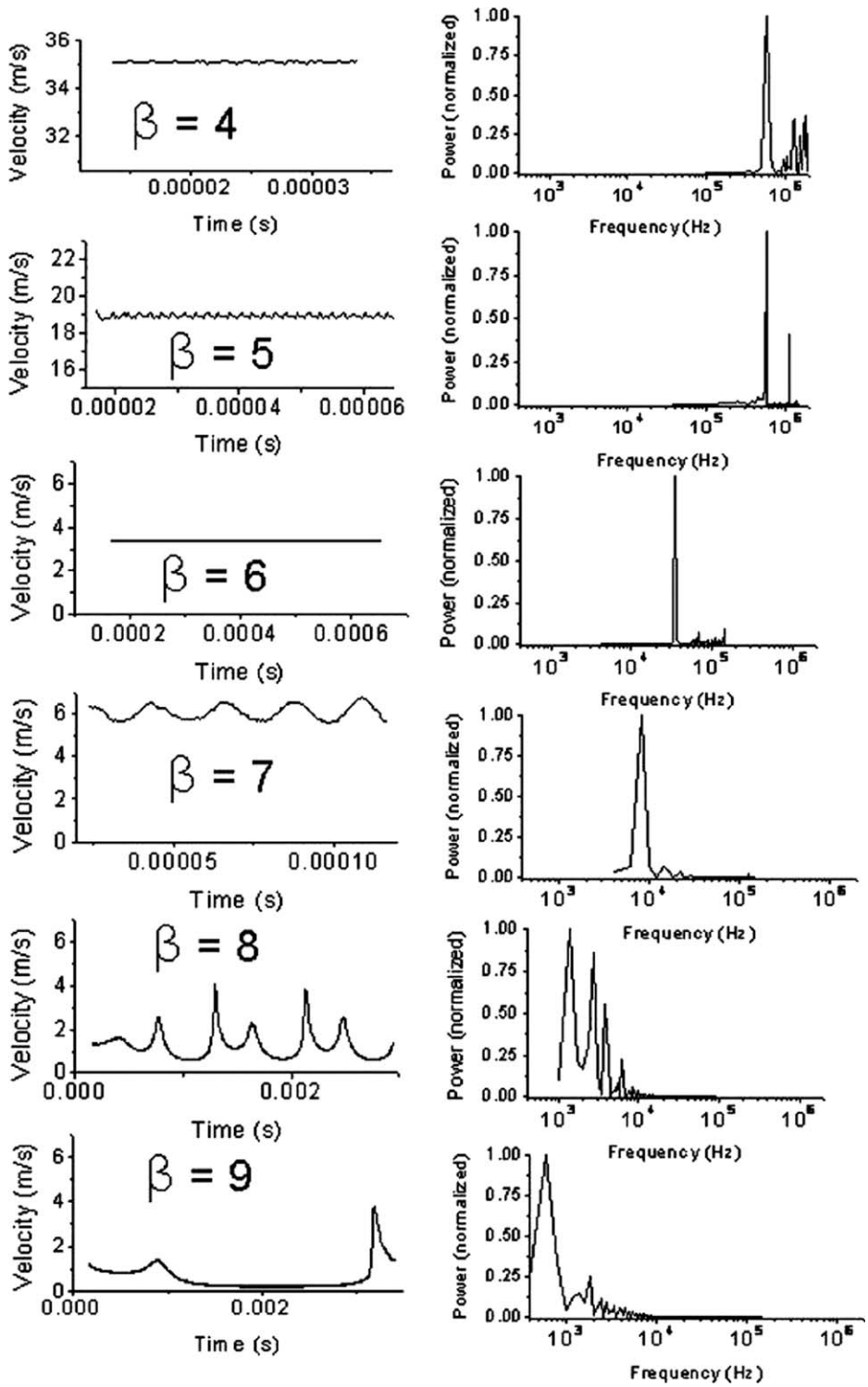

Figure 11. Variation of wave velocity over time and frequency spectra from different β values.[12]

Reproduced from Ref 12, with permission from American Chemical Society.

not involve changing chemical potential and thus lead us to a simplified equation for voltage generated as

$$V_{\mathrm{TE}} = \int_{x_{\mathrm{L}}}^{x_{\mathrm{R}}} \left(- \frac{L_{12}}{\sigma_{\mathrm{h}}} \nabla T \right) dx \sim \Gamma_{\mathrm{s}}(\Delta T) \tag{21}$$

The "excess power" observed during thermopower waves experiments was found to be correlated to doping in the CNTs. CNTs coated in fuels showed shifts in the G^- peak position of Raman spectra, correlated to changes in carrier concentration, which in turn affect the chemical potential. Excess power observed during thermopower waves can be described as

$$P_{\mathrm{xs}} = P_{\mathrm{out}} - P_{\mathrm{TE}} = \frac{V_{\mathrm{out}}^2}{R_{\mathrm{c}}} - \frac{V_{\mathrm{TE}}^2}{R_{\mathrm{c}}} \tag{22}$$

Here, V_{out} is the actual voltage output, V_{TE} is the thermoelectric prediction and R_{c} is the circuit load. The G^- peak position shifted by as much as 5 cm^{-1} when comparing

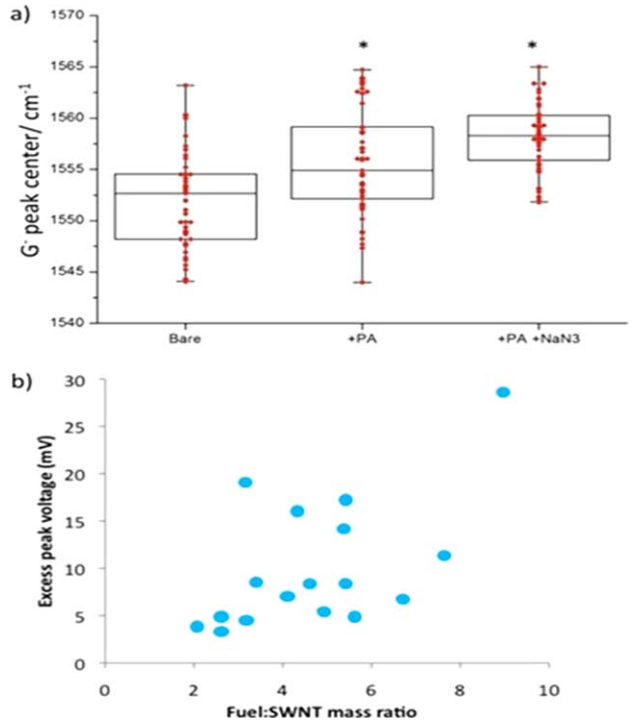

Figure 12. Excess thermopower from fuel doping.

(a) A shift of about 5 cm^{-1} in G^- peak position is observed on fuelling the CNTs (left to right). Boxes show the middle quartiles of the Raman measurements, and the arms show the maxima and minima. (b) Excess peak voltage generally increases with increased fuel loading (defined as ratio of fuel mass to SWNT mass), which could stem from increased doping from the fuel.[13] [Color figure can be viewed in the online issue, which is available at wileyonlinelibrary.com.]

fueled and bare CNTs, which translates to about 25 holes/μm doping and up to 100 mV additional voltage difference.[13] Figure 12 shows the shift in position of the G^- peak during the process of making thermopower devices. As can be seen, addition of the fuel picramide (PA) and the initiator (NaN_3) leads to a shift in the position of G^- peak. Also, from Figure 12, experiments studying the ratio of the mass of the adsorbed fuel to the mass of CNTs show a rough increasing trend for improved maximum voltage with increasing adsorption ratio.

Thus, a possible explanation for excess thermopower is that the change in chemical potential because of adsorption of the fuel followed by desorption during the chemical reaction leads to changing chemical potential across the electrical measurement terminals. A TWG exploits non-zero $\Delta\mu$ to lead to additional voltage output.[13]

The theory of excess thermopower tries to explain how the voltage generation of thermopower wave devices exceeds that of a comparable thermoelectric device and suggests methods for improving efficiency by suitably doping the conduits.

Conclusions

We have reviewed thermopower waves, a new approach to using chemical reactions to produce electricity. Current experiments have been predominantly carried out using highly exothermic fuels like TNA and nitrocellulose and conduits with high thermal and electrical conductivities. Experiments have been conducted exploring different fuels and conduits with varying thermal and electrical properties, which influence the voltage output's magnitude and oscillatory behavior. The logistic function was found to be a good analytical solution describing these self-propagating thermal waves. Thermopower waves look to be a promising technology for nanoscale power sources providing high power in short periods of time.

Literature Cited

1. Lewis L. Father of Chemical Engineering, Neal Amundson passes away 2011. Available at: http://www.egr.uh.edu/news/201102/father-chemical-engineering-neal-amundson-passes-away, accessed November 1, 2012.
2. Choi W, Abrahamson JT, Strano JM, Strano MS. Carbon nanotube-guided thermopower waves. *Mater Today*. 2010;13(10):22–33.
3. Choi W, Hong S, Abrahamson JT, et al. Chemically driven carbon-nanotube-guided thermopower waves. *Nat Mater*. 2010;9(5):423–429.
4. Abrahamson JT, Song C, Hu JH, et al. Synthesis and energy release of nitrobenzene-functionalized single-walled carbon nanotubes. *Chem Mater*. 2011;23(20):4557–4562.
5. Chakraborty AK, Coleman KS, Dhanak VR. The electronic fine structure of 4-nitrophenyl functionalized single-walled carbon nanotubes. *Nanotechnology*. 2009;20(15).
6. Walia S, Weber R, Latham K, et al. Oscillatory thermopower waves based on Bi_2Te_3 films. *Adv Funct Mater*. 2011;21(11):2072–2079.
7. Walia S, Weber R, Sriram S, et al. Sb_2Te_3 and Bi_2Te_3 based thermopower wave sources. *Energy Environ Sci*. 2011;4(9):3558–3564.
8. Walia S, Weber R, Balendhran S, et al. ZnO based thermopower wave sources. *Chem Commun*. 2012;48(60):7462–7464.
9. Abrahamson JT, Strano MS. Analytical solution to coupled chemical reaction and thermally diffusing systems: Applicability to self-propagating thermopower waves. *J Phys Chem Lett*. 2010;1(24):3514–3519.
10. Weber RO, Mercer GN, Sidhu HS, Gray BF. Combustion Waves for Gases (Le = 1) and Solids (Le $\rightarrow \infty$). *Proc Math Phys Eng Sci*. 1997;453(1960):1105–1118.
11. Zeldovich YB, Frank-Kamenetskii D. A theory of thermal propagation of flame. *Zh. Fiz. Khim*. 1938;12(1):100–105.
12. Abrahamson JT, Choi W, Schonenbach NS, et al. Wavefront velocity oscillations of carbon-nanotube-guided thermopower waves: Nanoscale alternating current sources. *ACS Nano*. 2010;5(1):367–375.
13. Abrahamson JT, Sampere B, Walsh MP, et al. Excess Thermopower and the Theory of Thermopower Waves. *Under review*.

Manuscript received Nov. 4, 2012, and revision received Apr. 8, 2013.